# Evaluation of the Enhanced Detection Capability of the Dual-Polarization Weather Radar

Reino Keränen[1], Jason Selzler[2], V. Chandrasekar[3]
[1] *Vaisala Oyj. Helsinki, Finland,* reino.keranen@vaisala.com
[2] *Vaisala Inc. Westford MA USA* jason.selzler@vaisala.com
[3] *Finnish Meteorological Institute, Finland*

(Dated: 3 June 2012)

## 1. Introduction

The elements of the complex signal covariance matrix $\boldsymbol{R}$ acquired by the dual-polarization weather radar provide for multiple means of detecting precipitation echo. A recently introduced approach uses the off-diagonal element $R_{hv}$ estimated by the cross-correlation function $\hat{R}_{hv}$ at lag-0. The precipitation echo power and subsequently the radar reflectivity are obtained from the magnitude of the cross-correlation function $\hat{R}_{hv}$. It has been shown to enhance the detection capability of precipitation by dual-polarization radars (Keränen and Chandrasekar, 2011).

This paper presents field evaluations of the procedure. We have evaluated the $|R_{hv}|$ based echo power estimator in varied meteorological conditions, in view of practical use cases. In typical operational conditions, the enhancement compensates the loss of 3 dB in signal-to-noise ratio acquired in the mode of simultaneous transmission in the H and V polarization channels ('STAR'), with respect to the mode of transmitting in the H channel, only ('H-only'). The detectability can be enhanced beyond this by the dedicated surveillance scans of enhanced detection capability.

Several applications of the enhanced surveillance scan can be envisaged. As known, the winter precipitation is often weak in echo power, and it has a shallow vertical structure. These reduce the detection range from the nominal capability in the warm season, and they lead to seasonally persistent gaps in the radar based observations in sparse networks. Mitigating the gaps of coverage in cool season can be attempted in the enhanced surveillance scans. In warm season, one is keen on detecting far distant weather systems as early as possible. Finally, additional margins of detectability serve for maintaining the coverage of observations subject to large rain induced attenuation in events of intense rain. In these applications, we are interested in enhanced detection, while not insisting that the dual-polarization variables are measured for precision uses in the full range.

These uses are explored as case studies of data samples acquired by the Vaisala C-band dual-polarization weather radars WRM200 in various climates. Data streams are available from all seasons from the development site of Kerava in Finland at high latitudes. Samples in tropical climate have been acquired at the operational site of Mateus Leme, near Belo Horizonte in Brazil. The $|R_{hv}|$ based echo estimator is available at these radars as a standard feature of the radar observations. The results from these two radars are presented to demonstrate the effectiveness of this new technology.

## 2. Enhanced detection capability at radars at varied climates

### 2.1 Shallow precipitation in cool season

We consider the radar coverages in large scale winter precipitation, observed by the Kerava radar in consecutive volume scans that are acquired within a period of nineteen minutes. In the bench mark sweep, total echo power is estimated from the autocorrelation $R_{hh}$ from 32 samples in the H-only mode. The sweep is preceded and followed by the scans in which echo power estimates of $R_{hh}$ and $|R_{hv}|$ are obtained from 32 pulses in the STAR mode. As usual in operational tasks, the moment data are summed through two range gates, leading to the effective range resolution of 500 m. There is a further pair of enhanced surveillance scans in which auto and cross correlation are summed from 128 pulses in consecutive16 gates, leading to the radial resolution of 4 km. Inspection of the sweep triplets (STAR, H-only, STAR) allow disentangling the effects of time evolution from the variability in detectability. The $R_{hh}$ echo power data are censored at the normalized total power $P_{hh}/N_{hh}$=1.5 dB, which yields less than one false alarm expected due noise in a sweep after applying speckle filters. An uncertainty of 0.5 dB in noise floors is allowed. The $|R_{hv}|$ echo data are censored at a threshold which leads to the equivalent false alarm rate. The rates have been validated by inspecting the clear sky bins at far ranges in higher elevation sweeps.

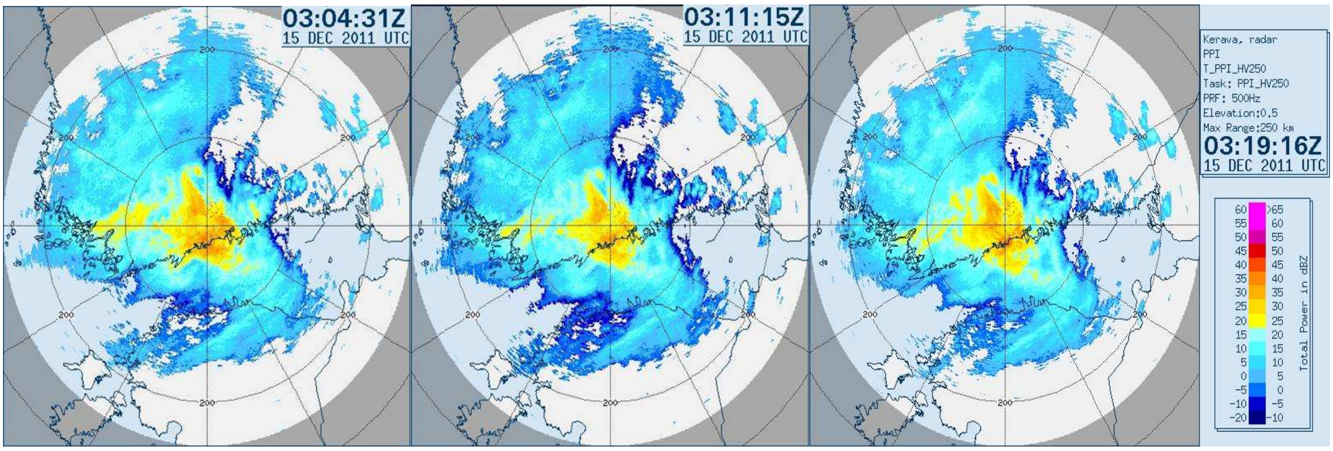


*Figure 1. Consecutive sweep data of total echo power ($R_{hh}$) in the STAR mode (left and right), and in the H-only mode (middle) in large scale precipitation. The autocorrelations are computed from 32 samples summed through two consecutive gates at the base gate spacing of 250 m. The pulse width is 2$\mu$s and the receiver band width is 0.6 MHz.*

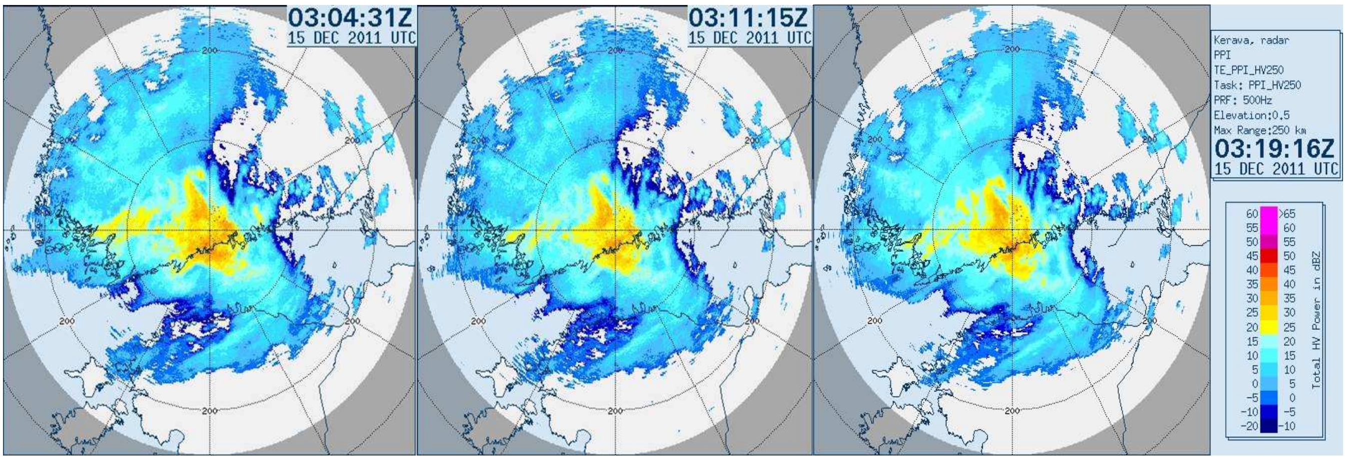


*Figure 2. As Figure 1 but with echo estimates from $|R_{hv}|$ in the STAR mode.*

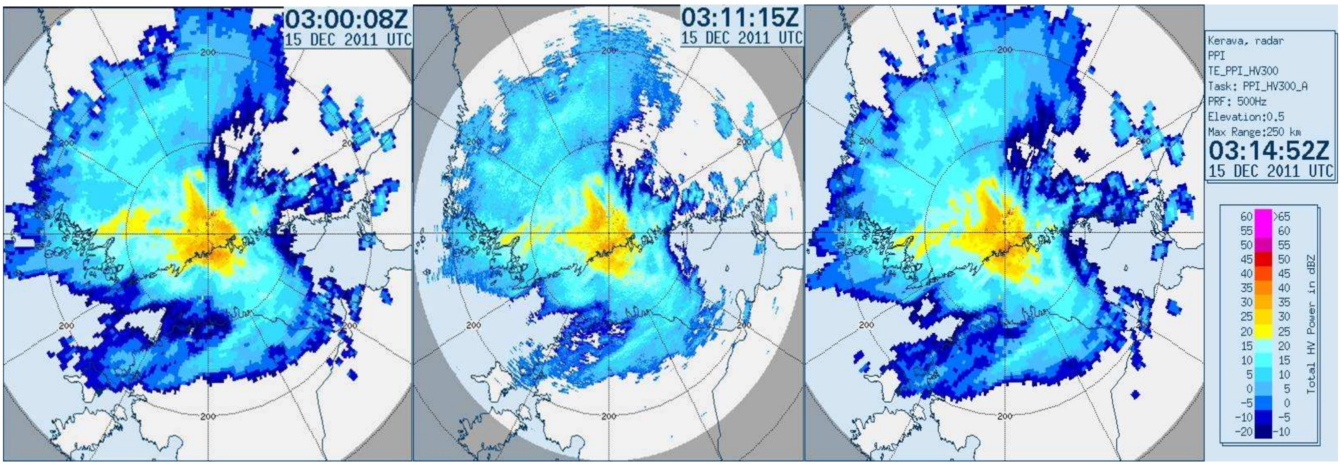


*Figure 3. As Figure 1 but the $|R_{hv}|$ based echoes are computed in the enhanced surveillance task in the STAR mode, in the left and in the right. Note the equal scales of distance.*

The comparisons of the $R_{hh}$ data, acquired at the elevation of 0.5$^o$, from 32 samples in the modes of STAR and H-only, are displayed in Figure 1. In careful inspection, the impact of the "3 dB" effect can be distinguished in the large scale precipitation echo. Similarly, the recovery effect of the $|R_{hv}|$ based echo power estimator can be distinguished in Figure 2.

Generally, the visible changes appear very minor, mostly due to the fact that fraction of edge echoes is small in large scale precipitation. This is consistent with previous findings (Scharfenberg K.A., et al. 2005). In contrast, the enhanced surveillance scans display significant areas of new precipitation based on the $|R_{hv}|$ echo power from a high number of samples, as shown in Figure 3. In closer look, these solid areas precipitation are in good match with the flaky detections in the 32 samples data.

For a quantitative evaluation of radar coverages, we observe that the enhanced surveillance mode serves well as the reference of 'precipitation', which can be used for computing the relative coverages of detection in the modes of STAR and H-only, using 32 samples. The relative coverages are summarized in Table 1. The STAR mode falls short by marginal two percent with respect to the H-only, when the $R_{hh}$ echo is considered. The marginal loss is recovered by the $|R_{hv}|$ echo, which brings the STAR coverage equal to the H-only mode. The fraction of weak echo may vary, thus events of higher marginal losses can be selected (Ivic, Melnikov, 2011), in which the weak echoes are expected to be recovered comparably, however.

| $R_{hh}$ STAR (Figure 1) | $R_{hh}$ H-only (Figure 1) | $\|R_{hv}\|$ STAR (Figure 2) |
|---|---|---|
| 0.89 | 0.91 | 0.91 |

*Table 1. The relative coverages of the precipitation echo computed from 32 samples in the modes of STAR and H-only, with respect to the reference set of* $|R_{hv}|$ *echo in the enhanced surveillance scans summing 128 pulses through 16 gates.*

The main outcome of this event evaluation is that the coverage of shallow precipitation is expanded by ten percent in the enhanced surveillance mode with respect to the legacy surveillances. This non-negligible enhancement translates into tens of kilometers improvement in the maximal range of coverage.

## 2.2 Detection of far distance weather systems

Surveillance is one of the primary tasks of weather radar, aiming at early detection of far distance weather systems. Despite the advances of global observing systems, such as satellites and lightning detection, ground based weather radars often provide the first, direct and timely observations of major weather systems developing at far distances. The Earth curvature and the vertical profiles of precipitation are strong constraints of the task. For any practical advance in the maximal detection range, the instrumental detectability must improve, significantly.

The enhanced surveillance with the $|R_{hv}|$ echo power appears well suited for expanding the detection range, at no instrumental cost. It is not a trade-off in surveillance to sum cross-correlation functions in range, because the radial dimension of the measurement volumes then matches with the transverse beam broadening at large distances. New observations are obtained through data reduction.

We consider a case of the warm season, observed by the Kerava radar. Initially, it is all fair weather, while a system of convective precipitation develops in the South. We follow up the development in the period of six hours, sampled with the enhanced surveillance scans every fifteen minutes. At the lowest elevation of $0.5^{\circ}$, the moment data are computed from 256 pulses, summed through sixteen consecutive gates at the base spacing of 250 m, resulting to the sampling of 4096 pulses at radial resolution of 4 km. The sweep time is about 20 seconds at the ray width of two degrees.

The echo data are censored for an equal image quality corresponding to the threshold of 2 dB in $P_{hh}/N_{hh}$ which is typical in conventional surveillance scans. For 256 pulses, the false alarms are suppressed to a rate less than one gate in a sweep, within the variability of 1.2 dB in the noise floors. These are too conservative in view of the optimal settings in the climate and for the hardware. They are chosen for the objective of quantifying the advantage of the enhanced surveillance with respect to the conventional surveillance scans.

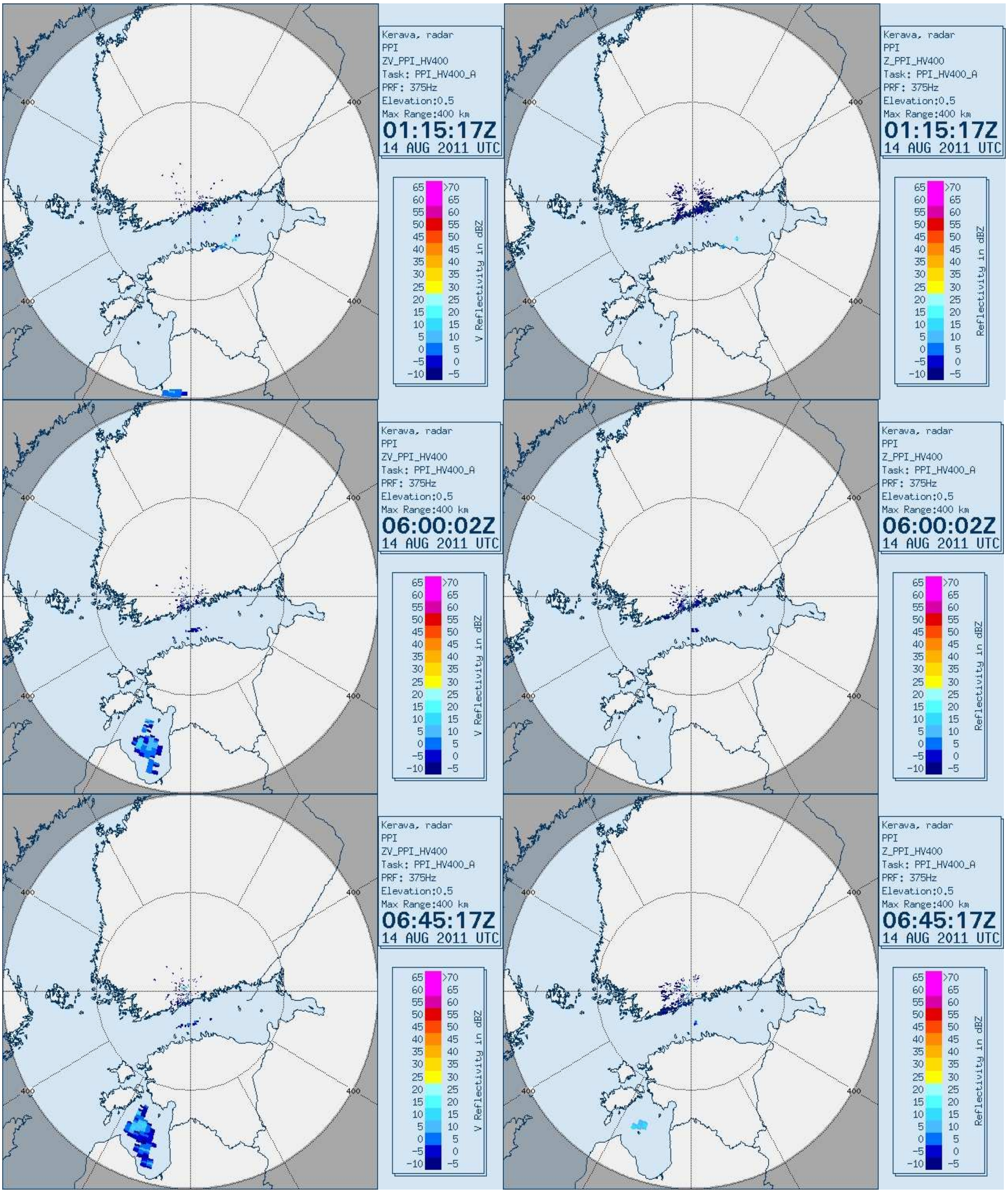


*Figure 4. An example of enhanced capability of detecting a far distance convective weather system. The left column: the fields of filtered reflectivity, estimated from the $|R_{hv}|$ echo power. The right column: the fields of filtered reflectivity from the $R_{hh}$ autocorrelation function using the same antenna voltages as input. Top row: the moment of first persistent $|R_{hv}|$ echo. The middle row: the last moment of no $R_{hh}$ echo. The bottom row: the moment of the first persistent $R_{hh}$ echo.*

Figure 4 displays the fields of reflectivity, filtered for ground clutter in three instances of the six hour period. The first instance is at 1:15 UTC when precipitation in the South is unambiguously detected as $|R_{hv}|$ echo. In fact, the first signals are seen 15 minutes earlier at the maximum range of 400 km, followed by persistent clusters of echo moving into North-West. At

1:15 UTC, no legacy echo is observed in the region. The second instance is at 6:00 UTC when the extent and intensity of the convective system have been evident in the $|R_{hv}|$ echo for hours, while the persistent echo is yet to be seen in the legacy echo. In the legacy surveillance mode, the convective weather system is detected as persistent echo at 6:45 UTC, which is five and a half hours later than the early detection in the enhanced surveillance mode. Such an advance in lead time is significant in events of major weather systems.

2.3 Enhanced detection capability in presence of rain induced attenuation in tropics

The $|R_{hv}|$ based echo estimator is operational in the Mateus Leme WRM200 radar. The site serves well as an example of modern C-band dual-polarization weather radar in the climatology of intense rain, which occurs seasonally. The radar runs a rapid scan scheduler of five minutes, which starts with a task optimized for dual-polarization observations of precipitation up to 250 km at the lowest elevations, followed by a task optimized for dual-PRF radial wind measurements at higher elevations. The volume base scan is complemented by the sweep of enhanced surveillance at the sampling of 1024, covering ranges up to 450 km. It is worth noting the scan fits in the multipurpose schedule of five minutes.

All the moment data are acquired in the STAR mode providing standard and dual-polarization moments at high quality. Reflectivity data are Doppler filtered for clutter, and they are corrected in real time for rain induced attenuation using the propagation term of the differential phase as a measure of attenuation. The propagation term is obtained as a step integrated in the adaptive method of the specific differential phase (Wang, Chandrasekar, 2009).

Tentatively, we select a weather case of large scale precipitation and inspect the results of the surveillance scan at the elevation of $0.5^{o}$, see Figure 5. Non-negligible rain induced attenuation can be inferred in the profiles of differential phase through rain into the North, up to the melting level at the altitude of 4 km which is reached at the range of 150 km. At the range of 260 km, the weakest precipitation is observed with reflectivity values of 8 dB, corrected for attenuation of 5 dB. Such echoes are typically interpreted as light precipitation, while the echoes are 1 dB in the units of signal-to-noise ratio (SNR), slightly above the level of censoring in the normalized total power $P_{hh}/N_{hh}$. Obviously, censoring occurs beyond that level, and one may ask if any area of significant precipitation echo is missed as too weak.

The fields of the $|R_{hv}|$ based echo estimator (Figure 5, bottom right) provide relevant new information about the attenuated echo. The range of detectable precipitation is expanded by additional 7 dB in these scan settings. Large areas of previously censored echo are now detected. They are here displayed as total unfiltered power, not corrected for attenuation. The fields of high co-polar correlation and the slowly evolving differential phase confirm that the pre-requisites of the $|R_{hv}|$ based echo estimator are maintained to the farthest distances of radar coverage. Most of the new echoes are estimated to less than 0 dBZ in units of reflectivity. Typically, they are insignificant precipitation, clouds and virga. However, the weakest echoes allow for recovering more significant precipitation in rays subject to large attenuation. In this event, the fields of $|R_{hv}|$ echo confirm that the area of significant precipitation to be recovered is negligible.

## 2. Summary

We have shown the results of the field evaluations and the applications of the enhanced reflectivity estimator, now operational at radars in two different climates. In typical operational dual-polarization tasks, it not only mitigates the 3-dB power loss in radar coverage, but provides additional observations of precipitation in enhanced surveillance scans. Such tasks are feasible even in the rapid run cycles. Non-negligible positive impacts are evident in the coverages of shallow winter precipitation and in lead times of early detection of far distance weather systems. The enhanced surveillance has potential to provide with additional margins to measure precipitation echo subject to high rain induced attenuation.

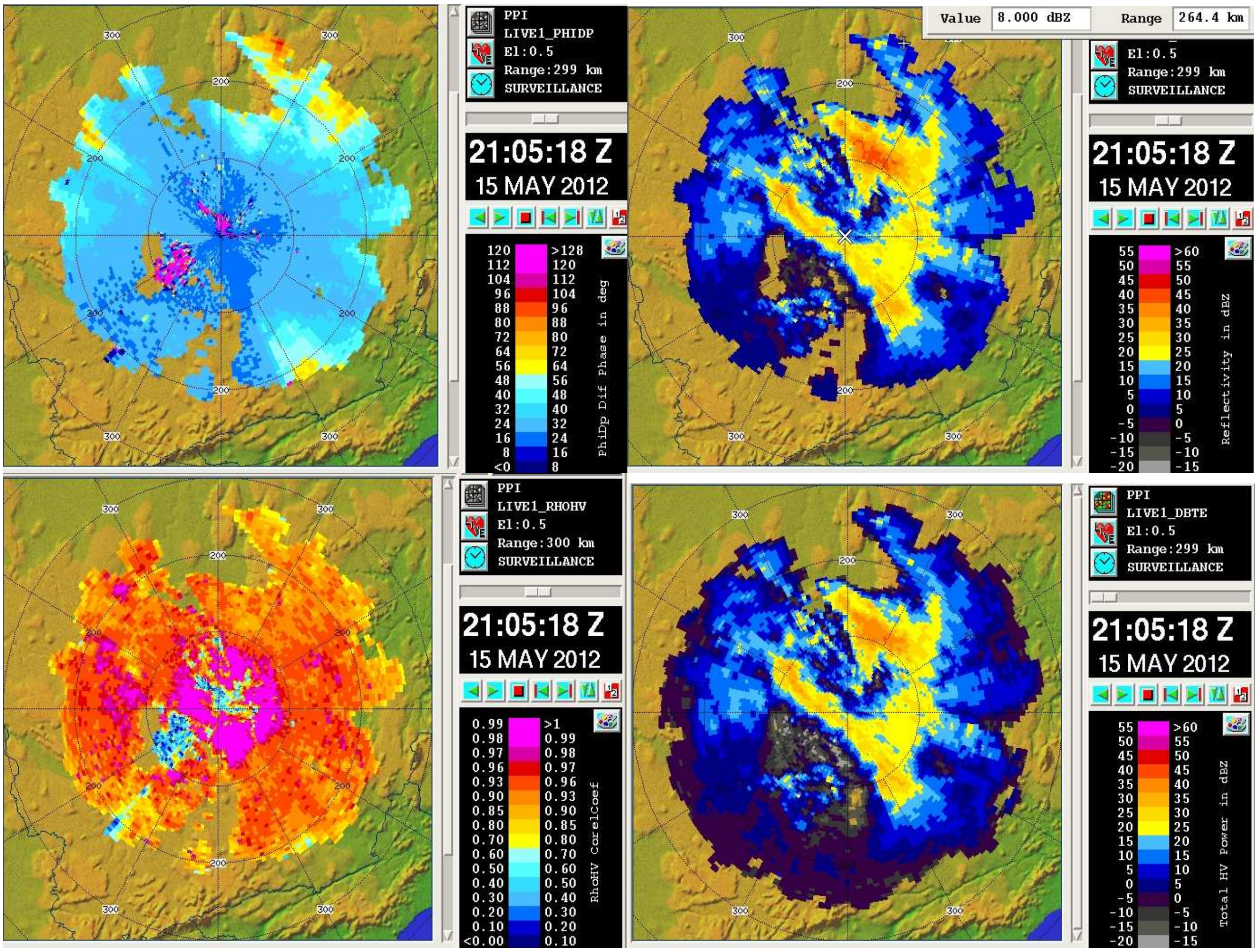


*Figure 5. An example of enhanced detection capability in an event of significant precipitation, with non-negligible rain induced attenuation in rays into the North. Top left: data fields of differential phase evolution, which quantify the rain induced attenuation up to the melting level at the altitude of 4 km, reached at the range of 150 km. Top right: filtered reflectivity ($R_{hh}$) corrected for attenuation; the cursor at the radius of 264 km, azimuth of 15$^o$ is at the edge of the precipitation subject to rain induced attenuation of 5 dB. Bottom left: data fields of co-polar correlation coefficient in precipitation (corrected for noise bias) displaying high values through all the precipitation. Bottom right: total echo power of the $|R_{hv}|$ estimator, providing with an enhancement of 7 dB in detection capability, in these run settings.*

## Acknowledgment

We acknowledge Lucio Black at Hobeco Sudamericana Ltda. for managing the Mateus Leme radar data sets.

## References

Keränen R., Chandrasekar V., 2010: Enhanced Detection Capability for Dual-Polarization Weather Radar. *The 35th Conference on Radar Meteorology,* Pittsburgh, U.S.A.

Scharfenberg K.A., Elmore K.L., Forren E., Melnikov V., and Zrnic D.S., 2005: Estimating the Impact of a 3-dB Sensitivity Loss on WSR-88D Data. *The 32nd Conference on Radar Meteorology,* Albuquerque, U.S.A.

Ivić I.R, Melnikov V., 2011: Combining the Coherency Based Detection and the 2D Despeckling to Improve Signal Detection in Dual-polarization Weather Radars. *The 35th Conference on Radar Meteorology,* Pittsburgh, U.S.A.

Wang Y., Chandrasekar V. 2009: Algorithm for Estimation of the Specific Differential Phase. *J. of Atmospheric and Oceanic Technology*, **26**, 2565-2578.